DETERMINING PIXL, SHERLOC, & SUPERCAM'S ABILITY TO IDENTIFY DOLOMITE PHASES & POTENTIAL BIOSIGNATURES IN CAMBRIAN MICROBIALITES. A. E. Murphy[1,2], M. Glamoclija[2], D. Blake[3], S. Sharma[4], L. W. Beegle[4], P. Sobron[5,6], K. Simon[5], D. Van Hoesen[5], S. Shkolyar[7,8], R. A. Yingst[1]. [1]Planetary Science Institute, 1700 E. Ft. Lowell, Suite 106, Tucson, AZ 85719 (amurphy@psi.edu), [2]Rutgers University, Newark, NJ 07102, [3]NASA Ames Research Center, Moffett Field, CA 94035, [4]NASA Jet Propulsion Laboratory, Pasadena, CA 91109, [5]Impossible Sensing, St. Louis, MO 63118, [6]SETI Institute, Mountain View, CA 94043, [7]NASA Goddard, Greenbelt, MD 20771, [8]Blue Marble Space Institute of Science, Seattle, WA 98154.

Introduction: One of the primary science goals of NASA's Mars 2020 mission is to search for potential biosignatures within and around Jezero crater [1,2]. Jezero crater is the only known location on Mars where carbonates are found in association with a paleolake [3], and the diversity of carbonate units in Jezero suggests there have been multiple periods of carbonate formation and alteration [4,5]. Of particular astrobiological interest is Jezero's western crater rim carbonates, or Marginal Carbonates, which are compositionally and topographically consistent with near-shore lacustrine carbonate deposits [4].

On Earth, such deposits provide high potential biosignature preservation. However, many terrestrial analogs use high resolution laboratory analyses to characterize biosignatures, which cannot be directly compared to data collected with the rover's instrument payload, making interpretations of martian data difficult. Therefore, we must characterize microbial biosignatures in terrestrial carbonates with comparable rover instruments and scales to better inform the Mars 2020 science team of what potential biosignatures in Jezero carbonates may look like.

Perseverance rover's payload includes instruments capable of fine-scale detection of minerals, organic molecules, and potential biosignatures, such as PIXL (Planetary Instrument for X-ray Lithochemistry), SHERLOC (Scanning Habitable Environments with Raman & Luminescence for Organics & Chemicals), and SuperCam's LIBS (Laser Induced Breakdown Spectroscopy) [6,7]. Instruments may be used to complement each other when investigating a martian sample, but when time, power, and data volume are limited, it is not always possible to deploy all the instruments on a single geologic target. Therefore, it is important to know which instruments may be most useful based on the geologic target to be investigated.

In this study, we apply instrumentation similar to that aboard the Mars 2020 rover, including Deep UV Raman and fluorescence, X-ray fluorescence (XRF), and LIBS to analyze previously characterized terrestrial samples from an ancient shallow marine environment [8]. The project's results are expected to help interpret rover-collected data and help target high potential biosignature samples for future sample return mission(s).

Materials: The Late Cambrian (515-500 Ma) Allentown Formation (New Jersey, USA) consists of supra- to sub-tidal paleoenvironments including tidal flat stromatolites, lagoonal thrombolites, and ooid shoals, which will serve as terrestrial analogs for microbial and non-microbial mediated carbonates. Although not lacustrine in origin, the original calcite/aragonite minerals were replaced by dolomite during burial diagenesis at temperatures from 260 - 322°C (±30°C) [8], making these samples a good analog for any shallow water Ca-carbonates on Mars that may have been altered by hot Mg-rich fluids. The formation is composed of three dolomite phases (microspar, zoned, saddle) that formed during different stages of diagenesis, resulting in varying crystal shape, size, and lithochemistry. The dolomites range from low Ca-excess to low Mg-excess and include trace elements Fe, Si, Mn, and Zn. Organic carbon is exclusively distributed within the first generation (microspar) of dolomite as observed by Raman D and G bands [8].

Rover-like Instrument Methods: *PIXL simulation*. PIXL-like data (~100 µm spot size) will be collected with the Mapping X-ray Fluorescence Spectrometer (MapX-III) at NASA Ames and compared to the previously collected commercial bench top µXRF results [9].

SHERLOC simulation. Deep UV (248.6 nm) Raman and fluorescence spectra will be collected at NASA JPL with the laboratory MOBIUS (40 µm spot size) and the flight analog BrassBoard (100 µm spot size) instruments to compare high resolution (laboratory) scans to lower resolution (rover-like) scans. High resolution, detail, and survey scans will be conducted on these samples to provide the closest possible comparisons to potential mission observations.

SuperCam LIBS simulation. LIBS data will be collected at Impossible Sensing with 50-100 µm resolution that will be artificially degraded (pixelated) to compare high resolution (laboratory) scans to lower resolution (rover-like) scans.

Preliminary Results and Discussion: Lanthanides (i.e., REEs) are detected in saddle dolomite using a µXRF commercial benchtop with (20 µm spot size) elemental maps (Fig. 1) and (200 µm spot size) line scans. The detection of lanthanides is an important finding because some (e.g., $CePO_4$ and

potentially Ce^{3+} substitution in other minerals) produce fluorescence in the same spectral region as organics [10], which could lead to identifying false potential biosignatures. In contrast, the first (microspar) dolomite phase appears relatively homogenous CaMg-carbonate with no obvious lanthanide detection. The microspar dolomite phase preserved organic carbon that is detectable with Raman spectroscopy [8]. Therefore, these samples make an excellent terrestrial analog for rover-derived SHERLOC data in that we may be able to observe the spectral signatures of organics and lanthanides in separate generations of dolomite within the same rock.

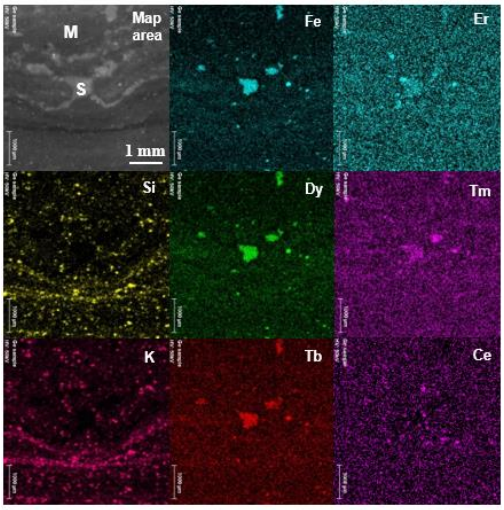

Fig. 1 *Selected µXRF elemental map results. The centered saddle dolomite (S, top left map area image) is rich in Fe and REE. The surrounding microspar (M) dolomite crystals are homogenous (Ca, Mg) with scattered quartz and feldspars (Si, K). Dark laminae near bottom of map is rich in Si, K. Map size is 5x5 mm with a spot size and step size of 20 µm.*

Additionally, the results from low resolution (200 µm spot size) line scans show that *Perseverance*'s PIXL instrument (120 µm spot size) can distinguish secondary mineral phases (saddle dolomite) from primary (microspar dolomite) mineral phases, which is important when interpreting a rock's alteration history and searching for potential biosignatures.

Further, the dolomites' Fe-content averages 0.3, 0.4, and 0.8 wt% Fe for microspar, zoned, and saddle phases, respectively [8]. Fe cations in carbonate phases cause significant UV absorption which hinders DUV Raman detection [11], therefore analyzing these samples may shed light on detectability limits of Fe-containing dolomite by DUV Raman.

Elemental imaging (≤60 µm spot size) with a µXRF commercial benchtop reveals the difference in texture and mineralogy of the organosedimentary structure (stromatolite) compared to the non-organic structure (tidal deposit) (Fig. 2B). PIXL and SHERLOC imaging (WATSON and ACI) can detect such features in a sample, and then target the microspar carbonate phase with SHERLOC's DUV Raman to search for organic carbon macromolecules.

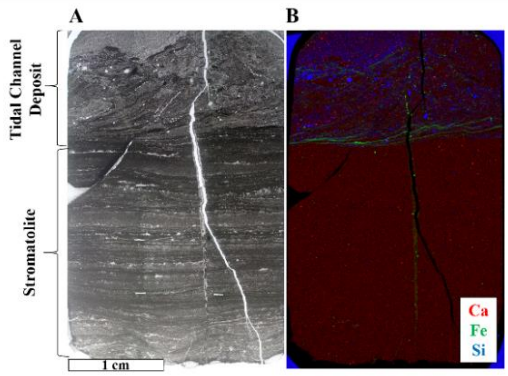

Fig. 2 *(A) Thin section of dolomitized Allentown stromatolite showing textural differences in organsedimentary deposit of a stromatolite, with fine laminae (bottom), compared to a non-biologically mediated tidal flat deposit (top). (B) µXRF map of (A). The stromatolite is composed of dolomite (red) and the tidal channel deposit exhibits iron-rich areas (green) and scattered feldspars (blue).*

Acknowledgments: Research supported by NASA NAI ENGIMA – Rutgers University and the Mars 2020 project.

References: [1] Williford, K. et al. (2018), Elsevier, 275-308. [2] Farley, K. et al. (2020) *Spa. Sci. Rev.*, *216*, 142. [3] Fassett, C. I. and Head, J. W. (2005) *Geophys. Res. Lett.*, *32*, L14201. [4] Horgan, B. H. N. et al. (2020) *Icarus*, *339*, 113526. [5] Zastrow, A. M. and Glotch, T. D. (2021) *Geophys. Res. Lett.*, *48*, e2020GL092365. [6] Allwood, A. C. et al. (2020) *Space Sci. Rev.*, *216*, 134. [7] Bhartia, R. et al. (2021) *Space Sci. Rev.*, *217*, 58. [8] Murphy, A. E. et al. (2020) *Sed. Geol.*, *410*, 105777. [9] Walroth, R. et al. (2022) in prep. [10] Shkolyar, S. et al. (2021) *Icarus*, *354*, 114093. [11] Morris, R. V. et al. (2022) LPSC.